Front. Optoelectron. China 2010, 3(1): 61–66
DOI 10.1007/s12200-009-0081-1

REVIEW ARTICLE

Optical fiber microwires and nanowires manufactured by modified flame brushing technique: properties and applications

G. BRAMBILLA (✉), Y. JUNG, F. RENNA

Optoelectronics Research Centre, University of Southampton, Southampton SO17 1BJ, UK

Abstract The modified "flame brushing" technique has been used to manufacture microwires and nanowires from both silica and compound glasses. In this paper, the properties of the wires manufactured by this technique are presented. Applications fabricated from microwires are also discussed.

Keywords optical micro- and nano-fibers (OMNF), microwire, nanowire, flame brushing

1 Introduction

Optical micro- and nano-fibers (OMNF) offer a number of exciting properties, including:

1) Large evanescent fields. For small radii, a considerable fraction of the transmitted power can propagate in the evanescent field outside the OMNF. High-Q resonators can be manufactured by knotting/coiling the OMNF on itself.

2) Low-loss interconnection to other optical fibers and fiberized components. Since OMNFs are fabricated by adiabatically stretching optical fibers, they preserve the original optical fiber dimensions at their input/output ends allowing low-loss splicing to standard fiberized components.

3) Robustness. Compared to their counterparts fabricated by etching or as growth from the liquid/vapor phase, optical OMNFs manufactured from optical fibers have a negligible surface roughness and thus superior mechanical strength.

Among the several methods used to manufacture OMNFs, the "modified flame brushing" technique [1] has proven to be the most versatile and provides OMNFs with the best physical properties. In this paper the mechanical and optical properties of OMNFs will be discussed, together with some recent applications.

Received August 1, 2009; accepted September 28, 2009

E-mail: gb2@orc.soton.ac.uk

2 Modified flame brushing technique

The flame brushing technique is probably the most widespread method for manufacturing tapers and couplers [2]. In this technique a gas burner acts as a point source heating only a very small section of the fiber fixed at its extremities to two translational stages. The burner travels in an oscillatory way, while the translational stages move apart. For the mass conservation, the diameter in the heated region decreases and by controlling the stages and the gas burner movements it is possible to achieve a specific taper profile [3]. Although this method is optimal for the manufacture of tapers from silica, it is not suitable for compound glasses. In addition, it introduces considerable amounts of hydroxyls in the heated glass because of the flame burning hydrocarbons.

The modified flame brushing technique [1] replaces the moving flame with a microheater (as shown in Fig. 1) and it can be used both to manufacture tapers from soft glasses

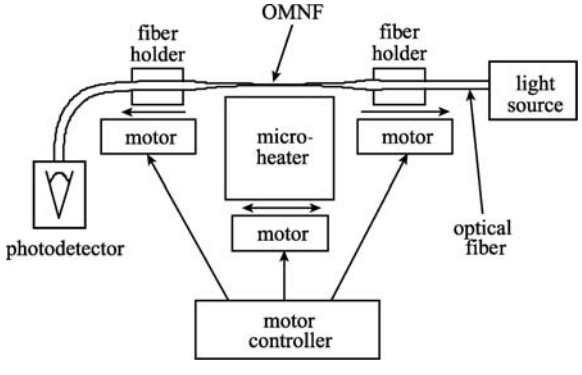

Fig. 1 Schematic of modified flame brushing technique set-up

[4] and to avoid any excess hydroxyls in the silica tapers/OMNF [5]. The microheater used in these experiments was manufactured by NTT-AT (Japan) [6], had a hot region smaller than 3 mm and could reach temperatures in excess of 170°C.

Silica OMNFs were fabricated from telecom optical fibers with 125 μm outer diameter. A schematic of the tapered fiber with an OMNF in the minimum waist region is shown in Fig. 2: The OMNF is attached to two fiber pigtails by two transition regions, which allow for easy handling of the OMNF without making use of nanomanipulators.

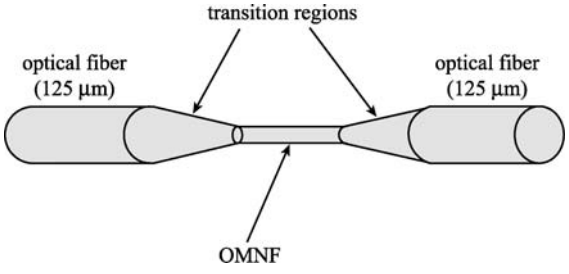

Fig. 2 Schematic of OMNF manufactured by modified flame brushing technique (OMNF is connected by two transition regions to conventional optical fibers)

The impurity level in silica OMNFs is given by the impurity level in the glass used as a cladding in optical fibers and by GeO_2 which is used to increase the glass refractive index in the fiber core and diffuses in the whole section during OMNF manufacture. Na, K, Ca, Mg, Al, Fe and Ti concentrations were estimated to be significantly smaller than 0.0001% mol while GeO_2 added an additional 0.02% mol impurity.

3 Physical properties

3.1 Mechanical properties

The ultimate strength σ_f (defined as the maximum stress a material can withstand) of silica OMNFs was measured by gradually increasing the weight at the lower extremity of the vertically held OMNF until fracture occurred [5]. The mass m responsible for the fracture was then measured using a high precision scale and σ_f was derived from the simple relation:

$$\sigma_f = \frac{m}{\pi r^2}. \quad (1)$$

The OMNF radius r was estimated using the mass conservation law and half of the samples were analyzed with a high resolution Scanning electron microscope (SEM) or a high magnification optical microscope to verify the accuracy of the estimation, which was within the experimental error (~3%). σ_f was evaluated on OMNF with radii (r) in the range 60 to 300 nm. Figure 3 shows that σ_f increases for decreasing r and it can exceed 15 GPa for $r < 100$ nm. This value is considerably higher than those recorded for conventional high strength materials (e.g., steel or Kevlar) and for bulk silica/optical fibers (σ_f~6 Gpa in air at room temperature) [7]. The increased strength observed in the silica OMNFs can be explained by a reduced possibility of having large cracks in small wires.

Griffith's fracture mechanics [8] predicts that a crack length of ~2 nm could be responsible for σ_f of the order of 20 GPa. In addition, since humidity is considered to be another cause of degradation of silica samples, OMNFs manufactured with a flame contain a considerable amount of hydroxyls (OH) and thus exhibit lower strength.

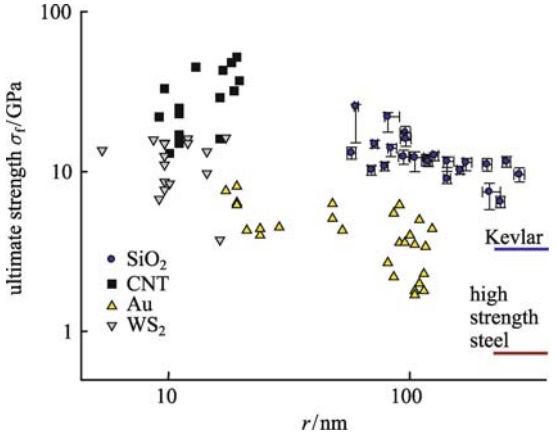

Fig. 3 Summary of ultimate strength (σ_f) measurements carried out on silica OMNFs (SiO_2) versus their radius r (Values of σ_f reported in the literature for high strength steel (A514), Kevlar, carbon nanotubes (CNTs), Au, and WS_2 nanowires are shown for reference)

3.2 Optical properties

The OMNF propagation loss was measured during fabrication using a monochromatic light source and a power meter connected to the fiberized pigtails. The good surface quality and lack of hydroxyls in OMNFs induced a low-transmission loss, which, at a wavelength $\lambda =$ 1.55 μm, is below 1 dB/m for radii of a few hundred nanometers [9]. This is comparable to the best results achieved with a common flame brushing technique utilizing flame burning hydrocarbons [10,11].

4 Applications

4.1 Mode filtering

The low transmission loss of OMNFs at small radii allows for light confinement with extremely low losses [1]: with adiabatic tapers, light at λ = 1.55 μm can be confined to micrometric spot sizes [10] with insertion losses smaller

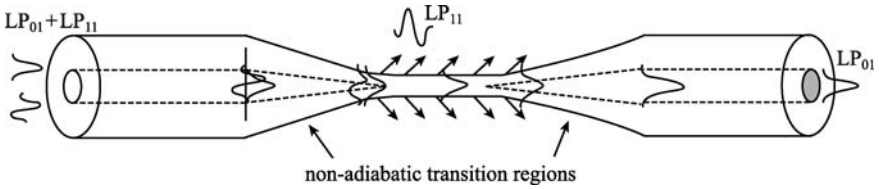

Fig. 4 Schematic of higher order mode filter (LP_{01} and LP_{11} represent fundamental and the first high-order modes, respectively)

than 0.1 dB. If the transition regions are adiabatic, guided modes launched in the core at one pigtail are continuously mode converted to guided cladding modes in the OMNF by the down-taper and then coupled back into guided core modes by the up-taper. On the contrary, when the transition regions are non-adiabatic, high-order modes are converted in even higher-order modes, which can be effectively suppressed by controlling the OMNF diameter (as shown in Fig. 4). For micrometric diameters, only few modes are guided [12], thus, using non-adiabatic transition regions, higher order modes can be selectively eliminated in the OMNF region [13]. The transition region geometry can be analytically derived from the adiabaticity criteria proposed by Love: the taper angle is supposed to be so small enough that the core modes can be considered unperturbed in their transition from core-guided to cladding-guided. In particular, at any fiber radius r the two modes having propagation constants β_1 and β_2 do not exchange power for distances larger than the beating length z. This results in the critical angle Ω being defined as

$$\Omega(r) = \frac{r}{z} = \frac{r(\beta_1 - \beta_2)}{2\pi}. \quad (2)$$

$\Omega(r)$ is different for different modes: LP_{01} and LP_{11} modes have critical $\Omega_{LP_{01}}(r)$ and $\Omega_{LP_{11}}(r)$ which are strongly dependent on r. The profile $\Omega(r)$ used in the higher mode filter shown in Fig. 4 is always smaller than $\Omega_{LP_{01}}(r)$ and occasionally greater than $\Omega_{LP_{11}}(r)$ for any chosen r. Figure 5 compares the transmission spectra of a common SMF-28 telecom fiber with and without the modal filter. The modal filter allows for single-mode operation in the whole 400–1700 nm range, avoiding the use of photonics crystal fibers [14].

In Fig. 5, the telecom fiber without modal filter (single-mode fiber, SMF) shows, for decreasing wavelengths, a clear output increase at specific wavelengths (shown as $\lambda_{c\_LP_{11}}$, $\lambda_{c\_LP_{21}}$, and $\lambda_{c\_LP_{02}}$); this is due to the guidance of higher order modes. The lack of these sudden increases has been ascribed to the presence of the sole fundamental mode at any wavelength. This has been confirmed by the observation of the far-field pattern with a 50 × microscopic lens and a charge coupled device (CCD) camera at the wavelength of a He-Ne laser (633 nm). When light is launched in a multimode fiber, guided modes travelling along the fiber interfere, resulting in the degradation of the

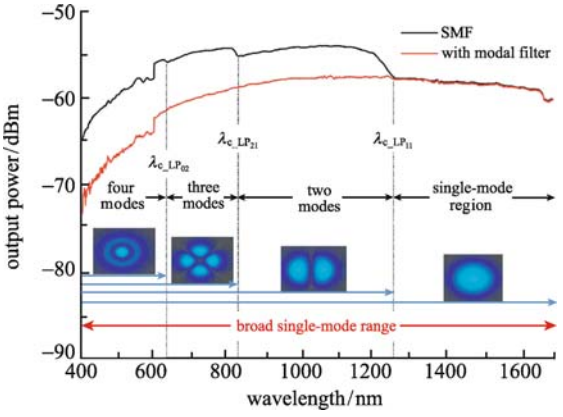

Fig. 5 Spectra of standard telecom optical fiber without (single-mode fiber, SMF) and with a modal filter ($\lambda_{c\_LP_{11}}$, $\lambda_{c\_LP_{21}}$, and $\lambda_{c\_LP_{02}}$ represent cutoff wavelengths for LP_{11}, LP_{21} and LP_{02} modes)

laser beam quality at the waveguide output (as shown in Figs. 6(a) and 6(b)).

Figures 6(c) and 6(d) show that when the modal filter is inserted, the single-mode guidance is indeed robust: the fiber output shows the sole fundamental mode even when bending is applied to the fiber: no mode conversion into higher order modes is observed. In addition, this scheme can be used to excite solely the fundamental mode in multimode fibers. If the tapering is performed at the splice point between a single-mode and multimode fiber, only the fundamental mode is excited in the multimode fiber [15]. Figure 7 shows the mode evolution in the tapered spliced fibers: light is launched in the core of the single-mode fiber; at the adiabatic down-taper the fundamental core mode of the SMF fiber ($LP_{01}^{core(SMF)}$) is converted into a guided cladding mode ($LP_{01}^{clad(SMF)}$), which then propagates unperturbed in the minimum waist region. $LP_{01}^{clad(SMF)}$ propagates along the splice joint with negligible loss ($LP_{01}^{clad(SMF)} \rightarrow LP_{01}^{clad(MMF)}$) and is then coupled back into the fundamental core mode in the multimode fiber (MMF) output fiber ($LP_{01}^{core(MMF)}$) by the adiabatic up-taper.

4.2 Efficient sub-wavelength light confinement

OMNFs have been shown to confine light in extremely small spot sizes [12] achieving nonlinearities up to 80000 times larger than those observed in silica telecom fibers

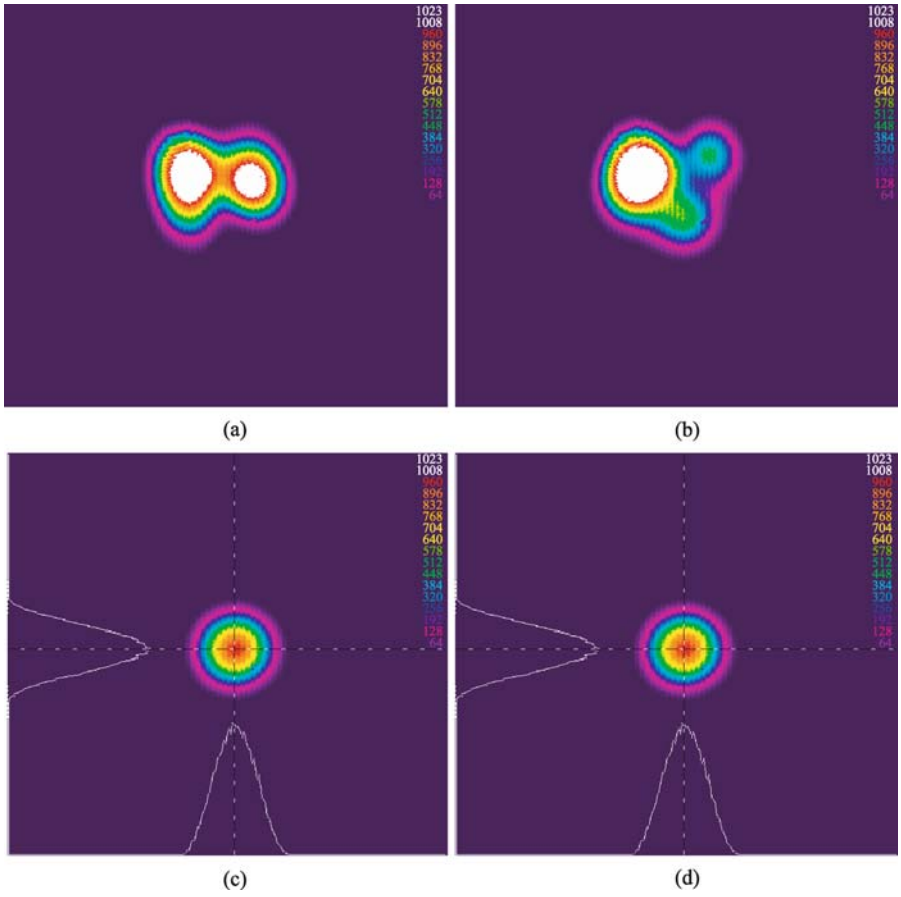

Fig. 6 Far-field imaging of SMF-28 fiber without ((a), (b)) and with ((c), (d)) mode filter at 632.8 nm (He-Ne laser) (Output has been collected for straight ((a), (c)) and bent ((b), (d)) fiber)

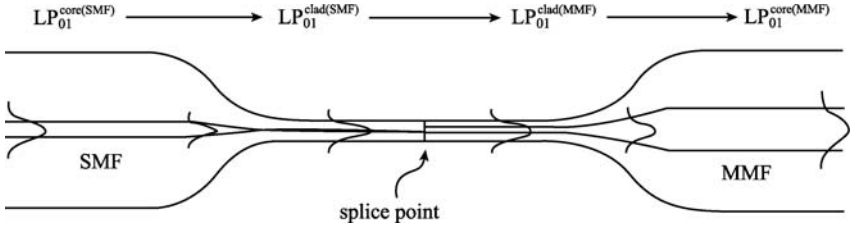

Fig. 7 Mode conversion in tapered splice between SMF and MMF ($LP_{01}^{core(SMF)}$, $LP_{01}^{clad(SMF)}$, $LP_{01}^{core(MMF)}$, and $LP_{01}^{clad(MMF)}$ represent fundamental modes propagating in core (core) or cladding (clad) of SMF or MMF fibers. Light is launched into SMF and collected from MMF)

[16]. Still, when light is confined into spot sizes comparable with the wavelength, diffraction occurs and the ultimate spot size Δx is related to the vacuum wavelength λ_0 and to the refractive index n of the medium where light propagates by the Heisenberg uncertainty principle [17]:

$$\Delta x \geqslant \frac{\lambda_0}{2n}. \tag{3}$$

Surface plasmon polaritons (SPPs) have been shown to be good candidates for sub-wavelength confinement because of their evanescent field nature. By nanostructuring the taper tip it is possible to excite SPPs efficiently and confine light to sub-wavelength spot sizes [17,18].

Figure 8(a) shows a schematic of the nanostructured device; it consists of an OMNF cleaved at an angle α and then coated with gold to excite SPPs; a small aperture is created at the very end of the tip to collect the output light.

The manufactured sample is shown in Fig. 8(b).

Its transmission properties were characterized as launching 400 fs, 50 nJ pulses in the wavelength range 650–1800 nm (supercontinuum source, Fianium, UK) and

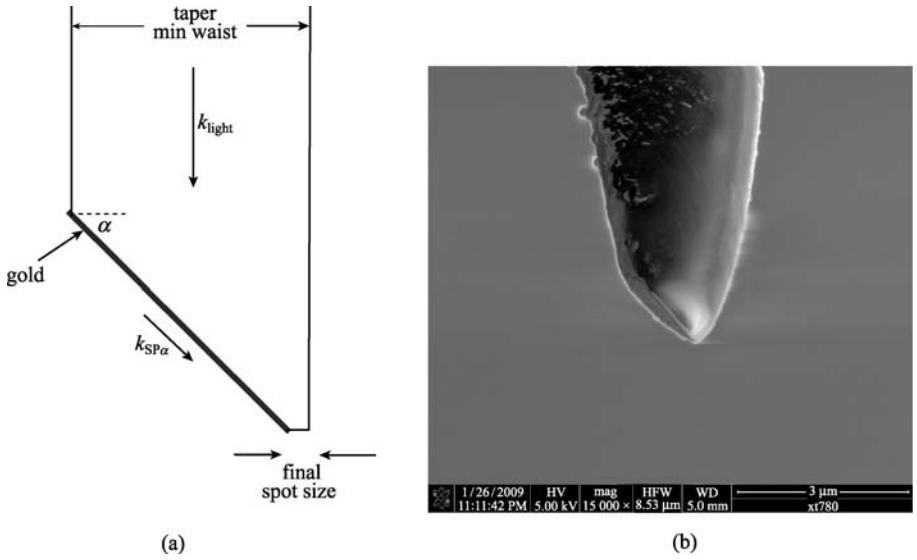

Fig. 8 Schematic (a) and SEM micrograph (b) of nanostructured OMNF tip for sub-wavelength confinement (tip is cut at an angle α and the angled surface is coated with gold. k_{light} and $k_{SP\alpha}$ represent the light propagation constant in OMNF and the component over α of surface plasmon propagation constant, respectively)

collecting the output light with a multimode fiber connected to an optical spectrum analyzer. Spectra of the source and of the transmission line were recorded to normalize the transmission results. Figure 9 shows the device normalized transmission spectrum. The maximum recorded transmission is ~ -11dB ($\approx 8\%$) at $\lambda = 780$ nm, nearly one order of magnitude higher than that simulated for pure geometrical reasons.

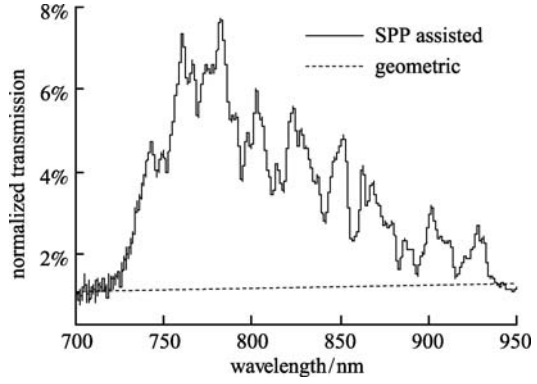

Fig. 9 Normalized transmission for device exploiting SPP (dashed line represents transmission observed because of simple geometrical considerations and it is shown for comparison)

5 Conclusion

In conclusion, microwires and nanowires manufactured by the modified flame brushing technique exhibit superior optical and mechanical properties to those manufactured by other techniques. Two groups of applications have been shown: 1) sub-wavelength light confinement exploiting surface Plasmon polaritons; and 2) mode filtering using non-adiabatic transition regions.

Acknowledgements G. Brambilla gratefully acknowledges the Royal Society for his research fellowship. The authors thank the Engineering and Physical Sciences Research Council (EPSRC, London, UK) for financial support, D. Payne, N. Zheludev, and K. MacDonald, for their helpful discussions and C. Cox for his help with the focused ion-beam (FIB) machine.

References

1. Brambilla G, Koizumi E, Feng X, Richardson D J. Compound-glass optical nanowires. Electronics Letters, 2005, 41(7): 400–402
2. Bilodeau F, Hill K O, Faucher S, Johnson D C. Low-loss highly overcoupled fused couplers: fabrication and sensitivity to external pressure. Journal of Lightwave Technology, 1988, 6(10): 1476–1482
3. Birks T A, Li Y W. The shape of fiber tapers. Journal of Lightwave Technology, 1992, 10(4): 432–438
4. Mägi E C, Fu L B, Nguyen H C, Lamont M R, Yeom D I, Eggleton B J. Enhanced Kerr nonlinearity in sub-wavelength diameter As_2Se_3 chalcogenide fiber tapers. Optics Express, 2007, 15(16): 10324–10329
5. Brambilla G, Payne D N. The ultimate strength of glass silica nanowires. Nano Letters, 2009, 9(2): 831–835
6. Takeuchi Y, Hirayama M, Sumida S, Kobayashi O. Characteristics of ceramic microheater for fiber coupler fabrication. Japanese Journal of Applied Physics, 1998, 37(6B): 3665–3668
7. Kurkjian C R, Krause J T, Paek U C. Tensile strength characteristics of “perfect” silica fibers. Journal De Physique Colloque, 1982, 43 (C-9): 585–586
8. Griffith A A. The phenomena of rupture and flow in solids.

Philosophical Transactions of the Royal Society of London, 1921, 221A: 163–198

9. Brambilla G, Xu F, Feng X. Fabrication of optical fibre nanowires and their optical and mechanical characterisation. Electronics Letters, 2006, 42(9): 517–519
10. Brambilla G, Xu F, Horak P, Jung Y, Koizumi F, Sessions N P, Koukharenko E, Feng X, Murugan G S, Wilkinson J S, Richardson D J. Optical fiber nanowires and microwires: fabrication and applications. Advances in Optics and Photonics, 2009, 1(1): 107–161
11. Leon-Saval S, Birks T, Wadsworth W, Russell P St J, Mason M. Supercontinuum generation in submicron fibre waveguides. Optics Express, 2004, 12(13): 2864–2869
12. Tong L, Lou J, Mazur E. Single-mode guiding properties of subwavelength-diameter silica and silicon wire waveguides. Optics Express, 2004, 12(6): 1025–1035
13. Jung Y, Brambilla G, Richardson D J. Broadband single-mode operation of standard optical fibers by using a sub-wavelength optical wire filter. Optics Express, 2008, 16(19): 14661–14667
14. Birks T A, Knight J C, Russell P St J. Endlessly single-mode photonic crystal fiber. Optics Letters, 1997, 22(13): 961–963
15. Jung Y, Jeong Y, Brambilla G, Richardson D J. Adiabatically tapered splice for selective excitation of the fundamental mode in a multimode fiber. Optics Letters, 2009, 34(15): 2369–2371
16. Yeom D I, Mägi E C, Lamont M R E, Roelens M A F, Fu L, Eggleton B J. Low-threshold supercontinuum generation in highly nonlinear chalcogenide nanowires. Optics Letters, 2008, 33(7): 660–662
17. Renna F, Cox D, Brambilla G. Efficient sub-wavelength light confinement using surface plasmon polaritons in tapered fibers. Optics Express, 2009, 17(9): 7658–7663
18. Renna F, Brambilla G, Cox D C. Light confinement in optical fibers using surface plasmon polaritons. IEEE Photonics Technology Letters, 2009, 21(20): 1508–1510